Korean J. Chem. Eng., **30**(5), 1058-1066 (2013)
DOI: 10.1007/s11814-012-0206-x

Evaluation of the performance of a commercial circulating fluidized bed boiler by using IEA-CFBC model: Effect of primary to secondary air ratio

Jong-Min Lee†, Dong-Won Kim, Jae-Sung Kim, Kyoungil Park, and Tae-Hee Lee

Green Energy Laboratory, Korea Electric Power Corporation (KEPCO) Research Institute, Daejeon 305-380, Korea
(*Received 13 July 2012 • accepted 26 November 2012*)

Abstract−The performance of a commercial circulating fluidized bed boiler in the Yeosu thermal power plant, which has been operating since October 2011 by KOSEP, has been evaluated by using the IEA-CFBC model. To validate the calculation procedure of the model, the calculated results were compared with the operation values such as the temperatures, pressures, emissions of SO_2 and NO, particles size distribution and unburned carbon fraction of the CFB boiler at a certain actual condition. The calculated results were comparable to measured values from the CFB boiler, so these could conform to acceptable formats with a good accuracy. The effect of the primary to secondary air ratio on the performance of the CFB boiler was also determined. As the primary air ratio increased, the solid fraction and temperature in the furnace freeboard increased. As a result, the solid circulation rate and the heat absorption in the furnace increased with increasing the PA ratio. In the case of the amount of heat absorption, the wall tube of the furnace absorbed much more generation heat in the furnace than the wing wall tube. The SO_2 emission decreased due to increase of the limestone hold up in the furnace, and the combustion efficiency somewhat increased with increasing the PA ratio. Therefore, from these results, we could expect to control the boiler performance such as the furnace temperature, steam temperatures of superheater or reheater, gaseous emissions and combustion efficiency through the changing the PA ratio of the CFB boiler.

Key words: Circulating Fluidized Bed, IEA-CFB Model, Primary Air Ratio, Yeosu Power Plant

INTRODUCTION

The use of high-quality coal has been getting limited attention in the electric power generation industry because of its increased price and lack of reserves. So, there has been increased interest in achieving effective coal utilization in a circulating fluidized bed (CFB) boiler, as its performance is superior to other boiler types in firing low value coals [1,2]. As a result of one of the successful ways to utilize low value coals, many CFB boilers were constructed and have been operated in the world [3]. Up to now, many 300 MWe CFB boilers have been put into commercial operation in China, the first supercritical 460 MWe CFB boiler has been put into operation at Lagisza Power Plant in Poland, and four units of 550 MWe CFB boilers at Samcheok Power Plant in Korea and a 600 MWe CFB boiler at Baima Power Plant in China are being erected [4,5]. However, there are few technical reports in terms of the performance of these large scale CFB boilers with changing the operation parameters, although there are a few reports in terms of commissioning experiences [4-7].

There are more than 20 units of CFB boilers in Korea in which most of them have been operated for cogeneration rather than for electric power generation only. Also, their capacities are less than 200 MWe and were designed to use high value coals as fuel, except a few boilers which have been constructed recently with firing low value coals [8]. So, in a bid to generate electric power efficiently, KOSEP (Korea South-East Power Company), which is one of subsidiaries of KEPCO (Korea Electric Power Corporation), decided to retrofit the #2 of Yeosu oil firing boiler with a CFB boiler. The design engineering and construction project of the Yeosu #2 CFB boiler, located in Yeosu city, Korea, was begun in July, 2009. In this project, Foster Wheeler designed a 340 MWe CFB boiler, firing sub-bituminous coal. Doosan Heavy Industries & Construction was responsible for the boiler equipment fabrication and procurement.

The Yeosu CFB boiler is different from recent CFB boilers in Korea. It is the largest CFB boiler and generates electric power only, which means that the steam quality, in terms of its temperature and pressure, is higher than other CFB boilers in Korea. The CFB boiler has been operated commercially since October 2011; however, there was apparently some room for optimization, particularly regarding the furnace temperature and the emission for SOx, which were sometimes not acceptable when compared with design values [9].

Therefore, we have simulated and evaluated the Yeosu CFB boiler to find how to control the ratio of primary air (PA) to primary and secondary air (PA+SA) to increase and stabilize its performance by using IEA-CFBC model. As a result of this simulation, we could expect to develop a good operation guide for the Yeosu CFB boiler.

IEA-CFBC MODEL

Many CFBC models have been developed since the early 1990's, based on the comprehensive bubbling fluidized bed combustion model. In the CFBC modeling approaches, there are different types of model, which can be distinguished as the global model, one-dimensional model (only gradients in vertical direction were considered), 1.5-dimensional model (a lateral distinction between core and

†To whom correspondence should be addressed.
E-mail: jmlee@kepri.re.kr

annulus was considered) and multi-dimensional model (computational fluid dynamics). The multi-dimensional model, which has been developed to some extent but is still in progress, is still far from mature because access to sufficient computational power, adequate for solution of the model, especially including the reactions of the CFB furnace, is limiting the use of CFD codes [10-12]. However, much work has been done, and some results have been applied to industrial CFB plants by modeling the CFBC with the 1- and 1.5-dimensional models [13,14]. Of these models, the IEA-CFBC model, developed by the mathematical modeling group in the IEA-FBC (International Energy Agency Fluidized Bed Conversion), offers a good approach for comprehensive and suitable modeling. Also, it has been applied to several industrial CFB plants and has shown good accuracy for prediction and evaluation of the performance of the CFB plants [15-17]. The IEA-CFBC model consists of several fields of mechanical, chemical and thermal processes, which are dependent on each other during the combustion processes in the CFB boiler. So, this model includes the following important fields [15,16]:

(a) Fluidization pattern of solid flow: the whole system is simplified as two axial zones: the dense bubbling bed, which might disappear for low solid inventory, and the freeboard zone, characterized by an exponentially decay in solid volume fraction. The shape of the transition zone in-between is calculated empirically [18,19]. Furthermore, the split between a lean core zone and a denser annulus is considered. The flow patterns are calculated individually for each size class, assuming a mono size distribution in the riser, and the individual results are superposed according to the mass fractions of the size classes.

(b) Development of particle size distribution: the fragmentation of particles, including coal, limestone and sand particles, due to the thermal shock is considered during their feeding into the furnace. Also, the attrition of these particles is considered during combustion, caused by mechanical stresses and uneven surface structures due to chemical reactions, which in turn shrink in diameter. The combination of these effects can establish a size distribution in the CFB boiler, which is much different from the particles initially fed.

(c) Gas flow: According to flow pattern calculations the gas is split into core, annulus and bubble flow which are balanced parallel and connected by gas exchange rate, calculated by dispersion approaches.

(d) Coal conversion: once into the furnace, the coal particles are heated and dried, and then are heated further and release volatiles, leaving a residue of carbon and ash, the char. These effects can happen in parallel to one another, which is considered by calculating the transient temperature profiles in the particles. Diffusion and reaction equilibrium, heat generation and particle release determine the char combustion rate and the particle temperature. The char concentration in the bed is balanced in turn with the oxygen concentration in the gas phase. The two concentrations are balanced in the surrounding iteration loop.

(e) Homogeneous and heterogeneous gas reaction: homogeneous gas reactions without any catalytic support of solid materials can be balanced straight in the gas phase. However, the effect of incomplete radial mixing of the gas cannot be modeled because of using one-dimensional approximation.

(f) Heat transfer: the main heat extraction occurs on the membrane walls in the upper part of the furnace. The calculation of the particle convection, which is one of the major parts of the heat transfer, is very sensitive towards the fluidization pattern since this determines the particles layer at the wall, which may be optically dense, reducing the radiative part.

The overview of the processes of this model is well presented in previous studies [15-17,20,21].

YEOSU CFB BOILER FEATURES

1. CFB Boiler Features

The Yeosu CFB combustor, shown in . 1(a), consists of a furnace, four compact cyclones and loopseals, coal and limestone feeding systems, primary and secondary air supplying systems and a convective backpass. The furnace (34 m (W)×8 m (L)×42 m (H)) has a rectangular footprint incorporating an aspect ratio of 4.25 : 1. The lower section of the furnace is tapered and covered with an ero-

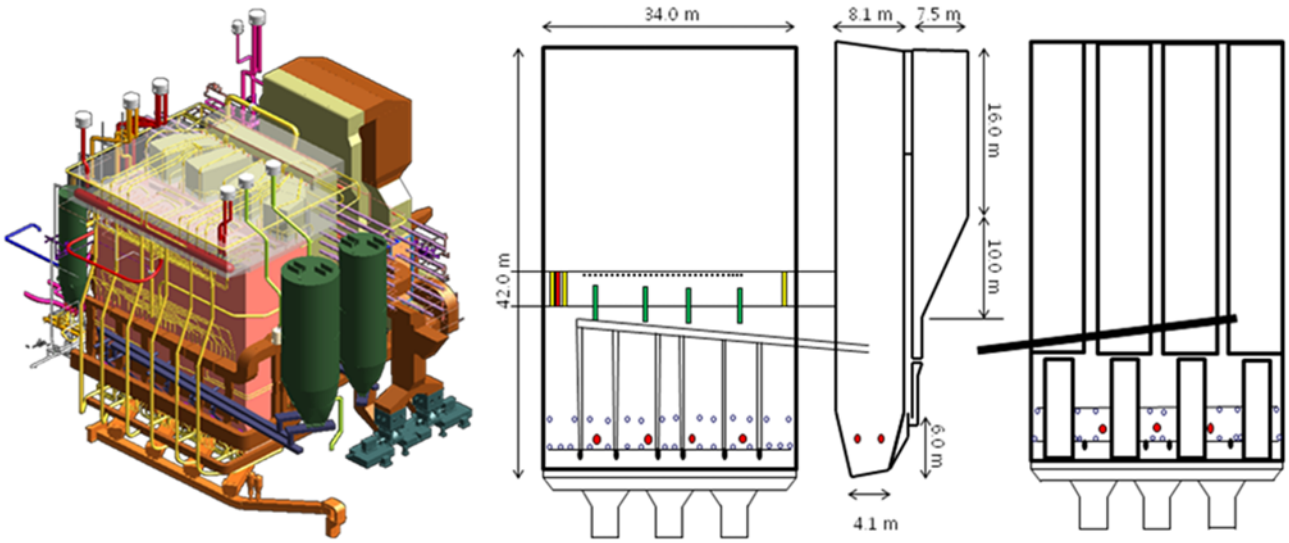

Fig. 1. Yeosu CFB boiler feature.

Table 1. Analyses of coal used in this study

Proximate analysis	wt% (Air dry basis)	Ultimate analysis	wt% (Dry basis)	Ash analysis	wt%
Moisture	20.00	C	71.50	SiO_2	33.45
Volatile matters	40.34	H	5.16	Al_2O_3	15.42
Fixed carbon	36.44	O	17.90	Fe_2O_3	11.03
Ash	3.22	N	1.19	CaO	21.11
Heating value	5,095	S	0.22	MgO	5.23
(LHV, kcal/kg)[a]		Ash	4.03	Na_2O	5.63
				K_2O	0.87
				SO_3	6.19
				TiO_2	0.66
				Others	0.41

[a]Calculated from Dulong equation: [81C+342.5(H-O/8)+22.5S-6(9H+W)], where, C+H+O+N+S+Water+Ash=100.0

sion resistant refractory, to a height of 6m from a distributor of the furnace. There are two division walls to realize a good fluidization in the furnace, which extend from the real wall (cyclone side) into the center of the furnace and can absorb the heat generated from the furnace. Also, there are several superheater (SH) and evaporator (EV) wing wall tubes in the furnace upper part, which can also absorb the heat generated from the furnace upper part.

Coal feed points were placed at both front (6-points) and rear (4-points) walls of the furnace lower section to allow for good fuel mixing, which was also able to be improved by taking a rectangular furnace with a wide aspect ratio. Limestone was injected through the secondary air injection ports which were aligned on upper and lower parts of the furnace front and rear walls. Also, sand particles, used as fluidizing bed material, were put into the furnace from a separate silo to maintain the bed inventory through several secondary air ports.

11-burners were installed on the furnace walls to heat the bed material to coal ignition temperature (≅500 °C) during start-up period of the boiler. Primary air for fluidization of the bed particles including coal, char, ash and sand particles was injected through the nozzles on the distributor of the furnace. The nozzles had an arrow type and a reasonable opening ratio for supplying even distribution of the injected primary air. Bottom ash was removed via four ash drain holes of the distributor, and was cooled on the conveyor system by cooling air. Most of discharged ash particles from the furnace were reused as bed materials after crushing and screening of them. Fly ash was finally captured by an electrostatic precipitator (EP) after going through the back pass, SCR and FGD systems in the power plant.

2. Properties of Coal, Limestone and Sand Particles

The analyses of the subbituminous coal used in this study are shown in Table 1. The coal contains 20.0% moisture, 40.3% volatile matter, 36.4% fixed carbon and 3.2% ash. The carbon and nitrogen contents are a little bit high and the ash and sulfur contents are relatively low in the coal. All the particles of the coal are under the size of 8.0 mm, as shown in Table 2. The limestone used in this study contains 86.6% $CaCO_3$ and 6.6% $MgCO_3$, and all the limestone particles are under the size of 1.2 mm. The size distribution of the limestone particles is shown in Table 2 with comparison to coal particles size distribution. The sand used as main bed material in the furnace has the particle density of 2,600 kg/m^3, and the size distribution of the sand is also shown in Table 2.

Table 2. Particle size distributions of coal, limestone and sand used in this study

Range (mm)	Coal (wt%)	Limestone (wt%)	Sand (wt%)
>8.0	0	0	0
4.000-8.000	10.7	0	0
2.000-4.000	24.7	0	0
1.400-2.000	16.8	0	0
1.000-1.400	14.1	0.3	0
0.710-1.000	11.7	13.5	0
0.500-0.710	8.4	15.3	0.1
0.355-0.500	4.6	7.4	37.0
0.250-0.355	3.0	7.9	38.5
0.180-0.250	2.0	10.2	13.5
0.125-0.180	2.0	19.2	7.4
0.075-0.125	1.0	19.9	2.4
<0.075	1.0	2.3	1.1

Table 3. Design operation conditions of the CFB boiler

Operation conditions	Values
Power generation [MWe]	100-340
PA flow rate [t/h]	440-730
SA flow rate [t/h]	260-530
Coal flow rate [t/h]	81-161
Limestone flow rate [kg/h]	4,000-5,600
Sand flow rate [kg/h]	970-1,800
Bed temperature [°C]	740-870
SO_2 emission [ppm @ air preheater]	<30
NOx emission [ppm @ air preheater]	<30

3. Operating Conditions and Modeling of the CFB Boiler

The design operation conditions of the Yeosu CFB boiler are shown in Table 3 with different loads of 30% MGR to BMCR. The CFB boiler can generate 340MWe at BMCR condition and turn down the load to 30% of the maximum rating. The emissions of SO_2 and NOx are designed below 30 ppm (@ 6% O_2 basis) through the control of limestone flow rate and the SCR process, respectively. Coal flow rates are in the range of 81 to 161 t/h, which are generally related to the flow rates of the air and the limestone and sand particles.

Table 4. Operation and simulation conditions with changing PA/[PA+SA] ratio

#[a]	Height [m]	Additional air flow rate [m^3/s]						
		PA ratio[b] [0.66]	PA ratio [0.46]	PA ratio [0.53]	PA ratio [0.60]	PA ratio [0.73]	PA ratio [0.80]	PA ratio [0.86]
1	0.0	188.01	178.28	181.52	184.77	191.25	194.49	197.74
2	0.60	5.26	5.26	5.26	5.26	5.26	5.26	5.26
3	1.50	9.04	9.04	9.04	9.04	9.04	9.04	9.04
4	2.00	41.20	38.30	39.27	40.23	42.16	42.13	44.10
5	2.50	19.33	19.33	19.33	19.33	19.33	19.33	19.33
6	5.00	29.08	52.99	45.02	37.05	21.11	13.14	5.17
7	9.95	1.46	1.46	1.46	1.46	1.46	1.46	1.46
8	41.7	0	0	0	0	0	0	0
9	Coal (kg/s)				43.01			
10	Limestone (kg/s)				4.70			
11	Sand (kg/s)				0.69			

[a]Air inlet position - #1: Primary air [PA], #2: Upper primary air [UPA], #3: Feeder(coal, limestone and sand) transport air, #4: Low secondary air [LSA], #5: Burner inlet air, #6: Upper secondary air [UPA], #7: Returned fluidizing air, #8 : Exit (top of the furnace), #9, 10, 11: coal, limestone and sand feed rate

[b]Actual operation condition based on 328 MWe power generation

To verify and predict the performance of the CFB boiler, the operation conditions were compiled from the Yeosu CFB boiler at a given condition of 328 MW electric power generation, as shown in Table 4. The various simulation conditions with changing the ratio of PA to (PA+SA) based on the compiled operation conditions are also shown in Table 4. With these conditions, the effect of the PA ratio on the performance of the CFB boiler was calculated by IEA-CFBC model. To verify the simulation results, the calculation data were compared with the measured data from the given operation condition of the CFB boiler, in which temperatures (at 0.4, 1.0, 4.0, 35.0 m) and pressures (at 0.25, 41.0 m) along the furnace, particle size distribution in the furnace, flue gas concentrations of SO_2 and NOx, and unburned carbon fraction in the fly ash were measured. However, since the Yeosu CFB boiler is a commercial one for electric power generation, the measurements were restricted to its accessible points. To measure the reliable data from the CFB boiler, measurement data of temperatures, pressures and flue gas concentrations were taken for an hour and averaged in this study. Other parameters used are shown in Table 5, according to some references and experimental measurements [22-27].

The sequence of calculation in the model study is as follows [15-17,20].

1. After initialization of the furnace geometry, the gas and solid properties and the fluid dynamic fundamentals were calculated. The input values were based on Tables 1, 2 and 4. Other important values used in this model are shown in Table 5.

2. A preliminary balance of fuel and air was performed.

3. After initial pre-balancing of an average size distribution function for estimation of the circulation rate, cyclone load and dense bed height, the real particle size distribution was balanced for each material such as coal, char and limestone.

4. Reactions such as dry, devolatilization, combustion and sulfur capture were linked to the particle phase and catalytic particle surfaces, where oxygen consumption and release of combustion products were also calculated and further reactions of the gas products were calculated in the gas phase.

5. The balances of solid and gas species concentration were solved independently, and both mass balances were adjusted in an iteration loop.

6. The energy released by the reactions with the heat flow and the heat transfer was balanced to yield the temperature profile in the riser. The feedback of the temperature to the reaction rate was

Table 5. Input data for calculation of IEA-CFBC model

Parameters	Coal	Char	Limestone	Sand
Density, [kg/m^3]	1,400	800	2,600	2,600
Sphericity [15], [-]	0.71	0.71	0.71	0.71
Heat capacity, [J/kgK]	840	600	840	840
Attrition constant [16], [1/m]	$2.0*10^{-6}$	$7.0*10^{-5}$	$1.0*10^{-6}$	$1.0*10^{-6}$
Fragmentation constant [17], [-]	3.0	1.0	1.0	1.0
Pre-exponential factor [18], [kg/m^2sPa]	-	0.79	-	-
Activation energy, E/R [18], [K]	-	8,000	-	-
Sulfation constant [19], [m/s]	-	-	0.075	-
Decay constant [20], a*u, [1/s]	6.0	6.0	6.0	6.0

considered in an iteration loop.

7. Pollutants were calculated in a post process, to avoid solution of all kinetic equations inside the iteration loops.

RESULTS AND DISCUSSION

1. Validation of the CFB Performance with a Commercial Operation Condition

The pressure and temperature profiles in the furnace calculated by IEA-CFBC model are shown in Fig. 2(a) and (b) with measured values from the CFB boiler. The pressure which means the solid fraction (hold-up) in the furnace decreased continuously with the furnace height and above about 2.0 m of the height the pressure decreased drastically, because the bed was changed from dense phase with 0.14 of the solid fraction to transition and dilute phases with 0.005 of the solid fraction as the furnace height increased. However, the axial pressure measurements were restricted to only two accessible points, because it is impossible to add the pressure measurement points on the furnace wall when considering the stable operation of the commercial CFB boiler. Although the measurement points of the pressure (at 0.25, 41.0 m) were absolutely small in number, the measurements showed a good agreement with calculated results in the bottom and the upper freeboard sections of the furnace. On the other hand, the axial pressure profile in the furnace could be estimated from the calculated results, although the verification might be insufficient, which had the similar trend of the previous study verified by IEA-CFBC model [17].

The temperature in the furnace as shown in Fig. 2(b) decreased

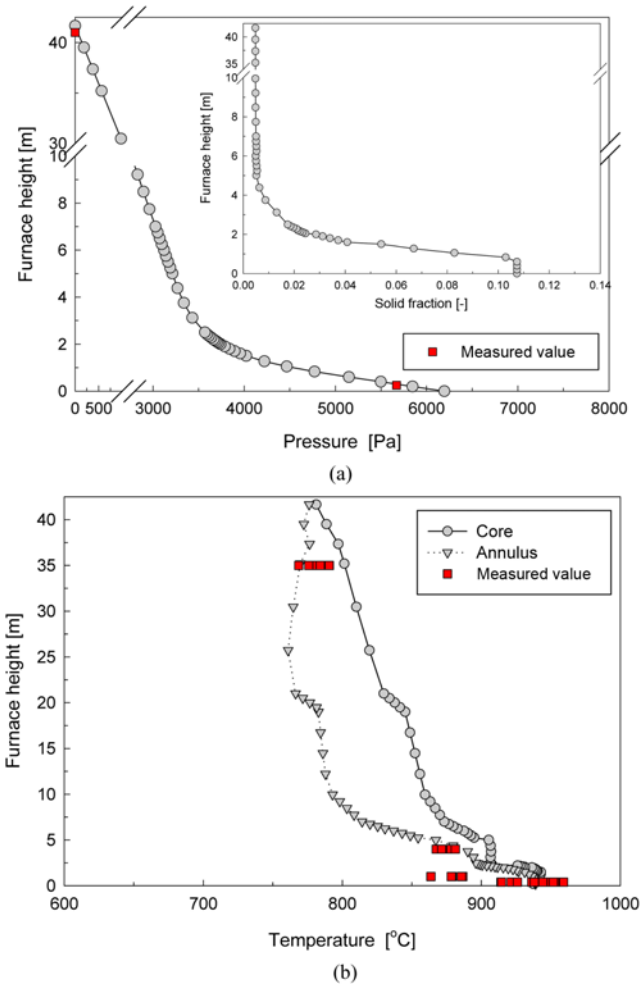

Fig. 2. Comparison of measured values with calculated values of (a) pressures and (b) temperatures in the CFB furnace.

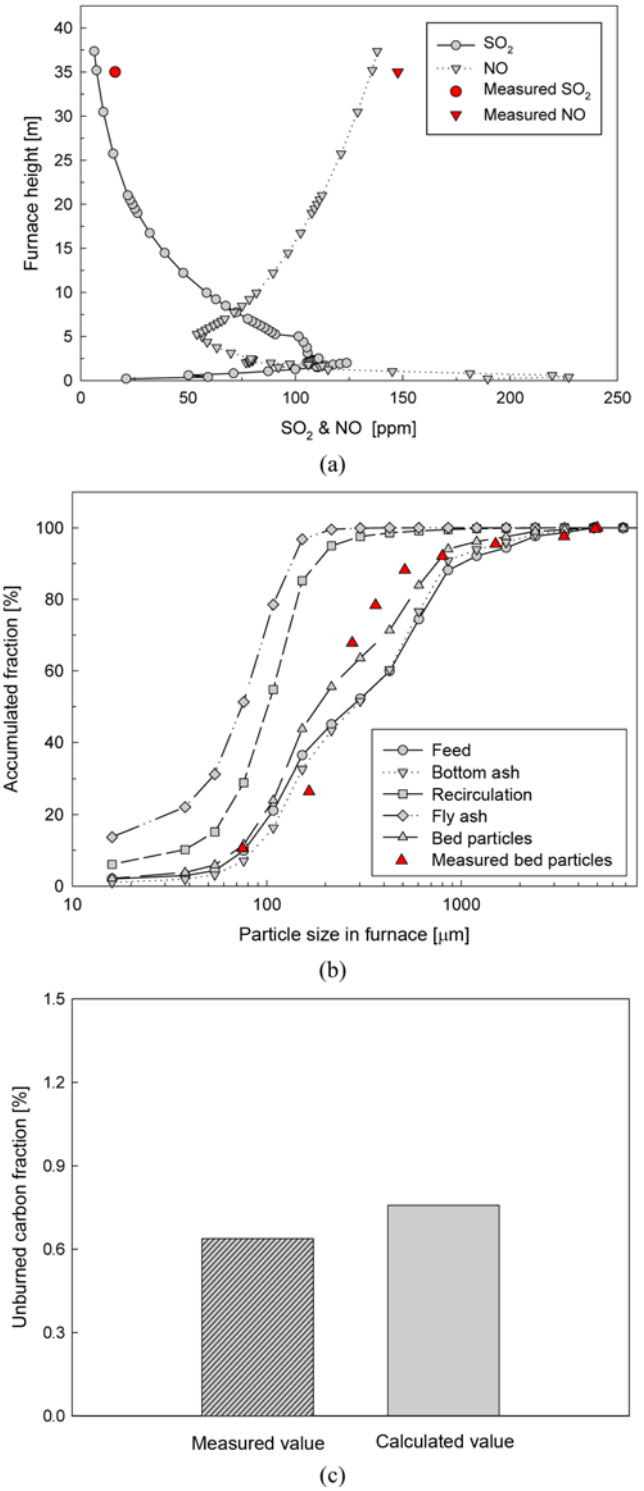

Fig. 3. Comparison of measured values with calculated values of (a) emissions of SO_2 and NO, (b) solid particle size distribution and (c) unburned carbon fraction in the CFB furnace.

from 950 °C to 800 °C with increasing the furnace height. This maybe comes from high volatile content and combustion reactivity of the coal and also from low solid circulation rate in this operation condition. So, the generated heat of combustion in the dense phase of the bed seemed to be transferred badly to the upper part of the furnace. In spite of that, the calculated values of the temperature along the furnace showed a good agreement with measured temperature values in the furnace.

On the other hand, the temperature profiles simulated in Fig. 2(b) were described as two distinctions between core and annulus regions of the furnace. In the IEA-CFBC model, it was considered that a clear distinction could be made between a dilute, upward flowing suspension in the core of the combustor and a descending annular layer at the walls, which is of higher density. So, the temperature profiles of the core and annulus regions based on the radial flow patterns of the furnace including the solid volume fractions and area fractions of the core and annulus regions were calculated with some assumptions and correlations proposed by several researchers [28-30]. The measured values from the furnace wall as shown in Fig. 2(b) had a better agreement with those of annulus region than that of core region, which implied that the core temperature might be much higher than measured values from the wall in the commercial scale CFB boiler.

The SO_2 and NO emissions in the flue gas, the particle size distribution in the bed and the unburned carbon in the fly ash were measured and compared with calculated values in Fig. 3(a), (b) and (c), respectively. According to the calculation results, the SO_2 concentration in the furnace continuously decreased after main sulfation reaction ($S+O_2=SO_2$) around the coal feeding point, and the SO_2 emission at the exit of the furnace showed about 11 ppm. The NO emission in the furnace showed a tendency to decrease in the dense and transition phase of the bed because of multi-injection of air via secondary air supplement, and then, showed a trend to increase continuously in the dilute phase of the bed along the furnace height. The measured values of SO_2 and NO in the flue were 16 ppm and 147 ppm, respectively, although these were somewhat higher than calculated, showed a good agreement with calculated values.

The particle size distribution in the bed was measured and compared with the calculated size distribution in Fig. 3(b) with other parts of the calculated particle size distribution of the boiler. Also, the unburned carbon fraction in the fly ash from the boiler is shown in Fig. 3(c) with comparing between calculated and measured values. From these results, we could validate that the calculated data by IEA-CFBC model conforms to acceptable formats with a good accuracy.

2. Effect of Primary to Secondary Air Ratio on the CFB Performance

To evaluate the effect of the ratio of PA to (PA+SA) on the performance of the CFB boiler, the calculation was carried out by IEA-CFBC model with changing the PA ratio from 0.46 to 0.86 based on the actual operation condition as shown in Table 3. The solid fraction (hold up) and temperature profiles in the furnace are shown in Fig. 4(a) and (b) with the PA ratio. The solid fraction in the dense phase of the bed decreased from 0.184 to 0.064 as the PA ratio increased, whereas the solid fraction in the dilute phase of the bed increased from 0.0022 to 0.0064. This might come from the increase of the solid up flow from the dense phase to the dilute phase due to

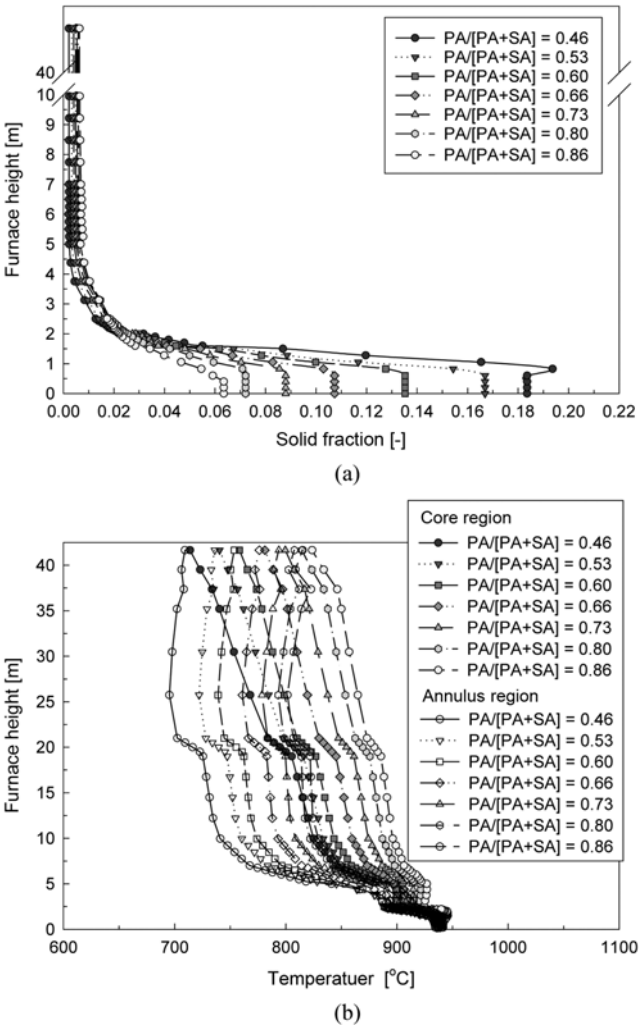

Fig. 4. Effects of PA/[PA+SA] ratio on (a) solid hold up and (b) temperatures in the CFB furnace.

the increase of carrying capacity of the solid particles in the dense phase as the PA ratio increased. The temperatures in the furnace exit increased from 710 °C to 823 °C as the PA ratio increased from 0.46 to 0.86 with nearly constant operating temperature in the bottom of the furnace as shown in Fig. 4(b). This implies that the difference between temperatures in the bottom and in the freeboard of the furnace decreased as the PA ratio increased. Moreover, as shown in Fig. 5(a) and (b), the solid down flow ratio, which means the mass ratio of solid up flow to solid down flow, decreased with increasing the PA ratio, although the ultimate gas velocity in the furnace freeboard was not changed. Therefore, the temperature and the solid hold up in the furnace can be controlled by changing the PA ratio at a constant total air flow rate.

The effects of the PA ratio on the carbon fraction and the volatile distribution in the furnace are shown in Fig. 6(a) and (b). The carbon fraction decreased with increasing the PA ratio, and was in the range of 0.011 to 0.049. This means that the combustion reaction of the char particles, which were formed from coal particles after devolatilization, much more occurred in the dense phase of the bed due to abundant O_2 resulting from increase of the PA ratio. However, the volatile concentration in the furnace increased with increas-

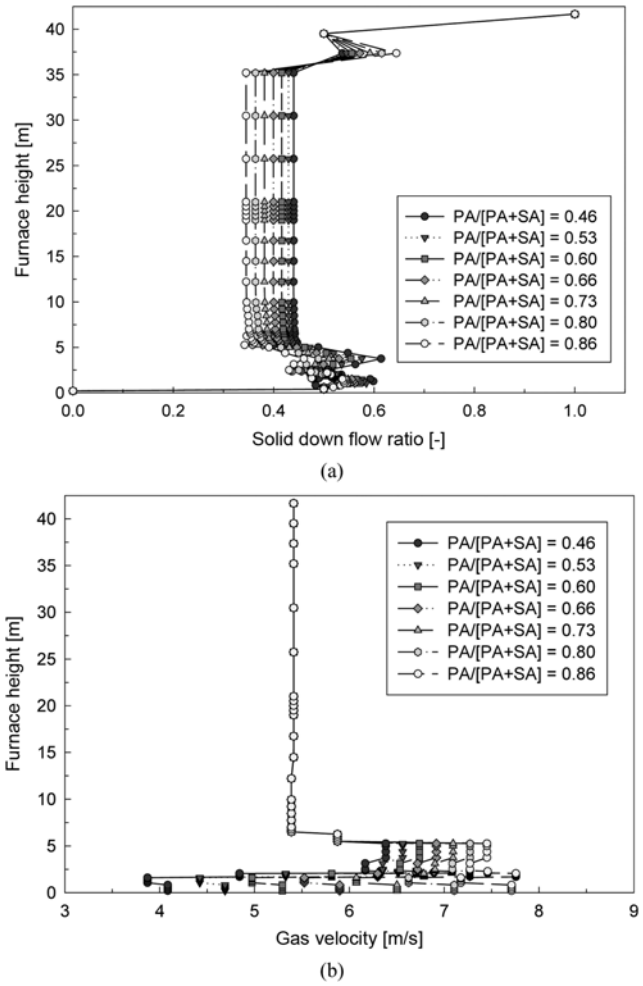

Fig. 5. Effects of PA/[PA+SA] ratio on (a) solid down flow ratio and (b) gas velocity in the CFB furnace.

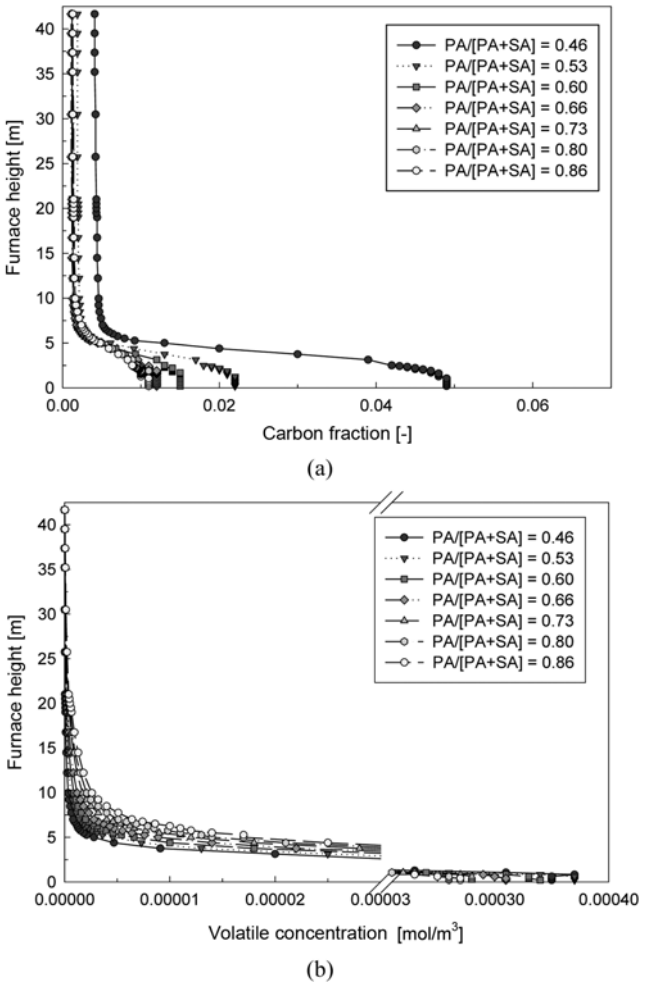

Fig. 6. Effects of PA/[PA+SA] ratio on (a) carbon fraction and (b) volatile concentration in the CFB furnace.

ing the PA ratio as shown in Fig. 6(b). This is because the O_2 supplied by the PA flow was consumed in large quantities for the carbon combustion in the lower part of the furnace; consequently, the volatile combustion occurred less in that region. So, the volatile matters remained uncombusted at the furnace height of about 20 m when the PA ratio was 0.86. These uncombusted volatile matters may keep the reduction atmosphere in the furnace, maybe, resulting in affecting the wall tube erosion in the furnace [31].

The emission gas concentrations of SO_2 and NO along the furnace are shown in Fig. 7(a) and (b), respectively, with changing the PA ratio. The SO_2 concentration along the furnace ultimately decreased above the dense phase of the bed, and also decreased with increasing the PA ratio in the furnace. This is because of the increase of solid hold up in the furnace with increasing the PA ratio, which means that there are many limestone particles for capture of SO_2 in the furnace. However, the NO concentration along the furnace showed a tendency to increase above the dense phase of the bed, and showed inconsistent results with increasing the PA ratio. This may come from the complicated NO formation and reduction reactions in the furnace [15,20].

The effects of the PA ratio on the solid circulation rate, the combustion efficiency and the heat absorption ratio in the furnace are shown in Fig. 8(a) and (b), respectively. The solid circulation rate increased more than five times in the range of the PA ratio from 0.46 to 0.86. The combustion efficiency showed a trend to increase drastically at the PA ratio of 0.46 to 0.60, and then the increase of the efficiency slowed down with increasing the PA ratio. On the other hand, the ratio of the heat absorption in the furnace to the heat absorption in the boiler backpass, which is represented as furnace heat duty in Fig. 8(b), increased as the PA ratio increased. This means that the increase of the solid hold up and temperature in the furnace improved the heat transfer coefficient in the furnace. Of the increase of the heat absorption in the furnace, much more heat absorption occurred to the furnace wall tubes rather than to wing wall tubes with increasing the PA ratio, as shown in Fig. 8(b) where heat-wall ratio and heat-tube ratio are represented as the ratio of heat absorption in the furnace wall tubes and the ratio of heat absorption in the wing wall tubes, respectively. This is because the heat transfer coefficient between the solid particles and the furnace wall tubes is generally larger than that between the solid particles and the wing wall tubes [32,33]. Therefore, we could expect to control the steam temperatures of the boiler such as superheater or reheater steam temperatures through the controlling the amount of heat absorption of the wall and wing wall tubes by changing the PA ratio of the CFB boiler.

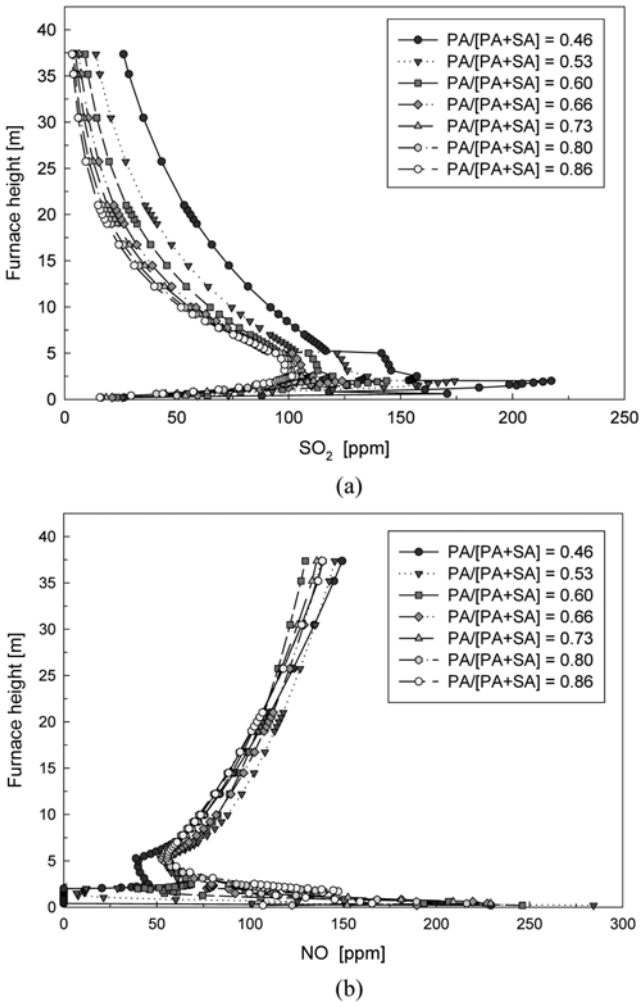

Fig. 7. Effects of PA/[PA+SA] ratio on (a) carbon fraction and (b) volatile concentration in the CFB furnace.

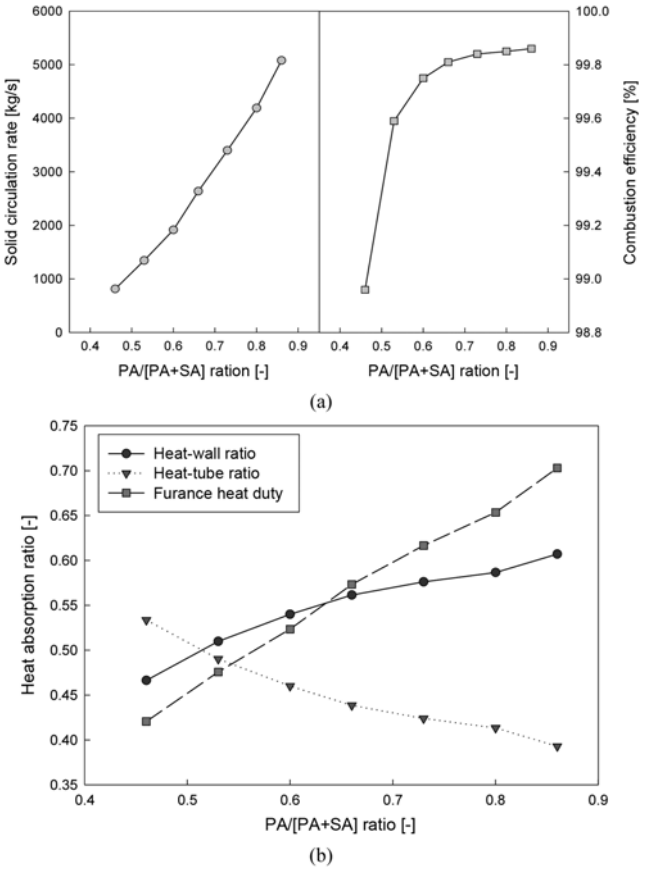

Fig. 8. Effects of PA/[PA+SA] ratio on (a) solid circulation rate and combustion efficiency, and (b) heat absorption ratio in the CFB furnace.

CONCLUSION

The simulation and evaluation of the Yeosu CFB boiler was performed to find how to control the primary air to secondary air ratio for the increase of the boiler performance by using the IEA-CFBC model. To validate the calculation procedure of the model, the calculated results were compared with the operation values such as the temperatures, pressures, emissions of SO_2 and NO, particles size distribution and unburned carbon fraction of the CFB boiler at a certain actual condition. The calculated results were comparable to measured values from the CFB boiler, so these could conform to acceptable formats with a good accuracy.

To evaluate the effect of the ratio of the primary air to secondary air flow rate on the performance of the CFB boiler, we also calculated changing the PA ratio from 0.46 to 0.86 based on the actual operation condition. As the PA ratio increased, the solid fraction and temperature in the furnace freeboard increased. As a result, the solid circulation rate and the heat absorption in the furnace increased with increasing the PA ratio. In the case of the amount of heat absorption, the wall tube of the furnace absorbed much more heat than the wing wall tube. On the other hand, the SO_2 emission decreased due to increase of the limestone hold up in the furnace, and the combustion efficiency somewhat increased with increasing the PA ratio. Therefore, we could expect to control the boiler performance such as the furnace temperature, steam temperatures, gaseous emissions and combustion efficiency through the changing the PA ratio of the CFB boiler.

REFERENCES

1. B. Leckner, *Therm. Sci.*, **11**, 5 (2007).
2. J. Koornneef, M. Junginger and A. Faaij, *Progress in Energy Combus. Sci.*, **33**, 19 (2007).
3. B. Leckner, *Developments in fluidized bed conversion during 2005-2010*, IEA-FBC Report, Chalmers University of Technology Press, Sweden (2011).
4. M. Zhan, H. Wu, Y. Sun and Q. Lu, 21st International Conference on Fluidized Bed Combustion, Naples, Italy, 107 (2012).
5. J. Utt and R. Giglio, Power-Gen India & Central Asia Conference, New Delhi, India, 3 (2012).
6. W. Nowak, R. Walkowiak, T. Ozimowski, J. Jablonski and J. Wyszynski, *9th International Conference on Circulating Fluidized Beds,* Hamburg, Germany, 1057 (2008).
7. T. Jantti and R. Parkkonen, Power Gen Asia, Bangkok, Thailand (2009).
8. J. M. Lee, D. W. Kim and J. S. Kim, *Korean J. Chem. Eng.*, **28**(8), 1791 (2011).

9. D. W. Kim, J. M. Lee, K. I. Park, T. H. Lee and J. S. Kim, *Proceedings of 2012 KIChE Spring Meeting*, 311 (2012).
10. J. W. Pritchett, T. R. Blake and S. K. Garg, *AIChE Symp. Ser.*, **74**, 134 (1978).
11. A. Boemer, H. Qi and U. Renz, Proceedings of the 29th IEA-FBC Meeting, Paris, France (1994).
12. D. Pallares, M. Palonen, V. Yla-Outinen and F. Johnsson, Proceedings of the 21th International Conference on FBC, Naples, Italy, 867 (2012).
13. S. Mori, K. Narukawa, I. Yamada, T. Takebayashi, H. Tanii, Y. Tomoyasu and T. Mii, *Proceedings of the 11th International Conference on FBC*, Montreal, Canada, 1261 (1991).
14. L. Zhang, T. D. Li, Q. Y. Zhen and C. D. Lu, *Proceedings of the 11th International Conference on FBC*, Montreal, Canada, 1289 (1991).
15. J. P. Hannes, *Mathematical modeling of circulating fluidized bed combustion*, PhD Thesis, Delft University of Technology, The Netherlands (1996).
16. J. M. Lee and J. S. Kim, *Korean J. Chem. Eng.*, **16**(5), 640 (1999).
17. J. M. Lee, J. S. Kim and J. J. Kim, *Energy*, **28**, 575 (2003).
18. Y. C. Wen and L. H. Chen, *AIChE J.*, **6**, 117 (1982).
19. K. E. Wirth, *Chem. Eng. Technol.*, **11**, 11 (1988).
20. J. P. Hannes, C. M. Bleek and U. Renz, *Proceedings of the 13th International Conference on Fluidized Bed Combustion*, Orlando, Florida, 287 (1995).
21. J. M. Lee and J. S. Kim, *Korean Chem. Eng. Res.*, **38**(1), 53 (2000).
22. S. Ergun, *Chem. Eng. Prog.*, **48**, 89 (1952).
23. D. Merrick and J. Highley, *AIChE Symp. Ser.*, **70**(137), 366 (1974).
24. D. Bellgardt, F. Hembach, M. Schoessler and J. Werther, Proceedings of the 9th International Conference on FBC, Boston, 713 (1987).
25. I. W. Smith, *Fuel*, **57**, 409 (1978).
26. E. H. P. Wolff, *Regenerative sulfur capture in fluidized bed combustion of coal*, PhD Thesis, Delft University of Technology, The Netherlands (1991).
27. D. Kunii and O. Levenspiel, Fluidization Engineering 2nd Ed., Butterworth-Heinemann (1991).
28. M. Seiter, *Radial solid concentration and axial solid concentration in near wall areas circulating fluidized bed*, PhD Thesis, Erlangen, Germany (1990).
29. C. M. H. Brereton and J. R. Grace, *Chem. Eng. Sci.*, **48**(14), 2565 (1993).
30. A. Glatzer, *Solid distribution and heat transfer by radiation in circulating fluidized bed*, PhD Thesis, Vienna University, Austria (1994).
31. J. M. Lee, D. W. Kim and J. S. Kim, *Operation analysis and guide for the Yeosu CFB boiler*, Technical Report (TM K02P2011), KEPRI, Korea (2011).
32. E. J. Gottung and S. L. Darling, *Proceedings of the 10th International Conference on FBC*, New York, 617 (1989).
33. P. Basu, *Combustion and gasification in fluidized beds*, CRC Press, Taylor & Francis Group, New York (2006).